

Supporting information

Growth of Au Nanoparticles on Phosphorylated Zein Protein Particles Used as Biomimetic Catalysts for Cascade Reactions at Oil-Water Interface

Yongkang Xi ^{a1}, Bo Liu ^{a1}, Shuxin Wang^a, Xiaonan Huang^a, Hang Jiang^b, Shouwei Yin ^{a, c, d*}, To Ngai^{b*}, Xiao-Quan Yang^a

^a Research and Development Center of Food Proteins, Guangdong Province Key Laboratory for Green Processing of Natural Products and Product Safety, School of Food Science and Engineering, South China University of Technology, Guangzhou 510640, PR China

^b Department of Chemistry, The Chinese University of Hong Kong, Shatin, N.T., Hong Kong

^c Sino-Singapore International Joint Research Institute, Guangzhou 510640, PR China

^d Research Institute for Food Nutrition and Human Health, Guangzhou, China

* Corresponding author

Yin, S. W. E-mail: feysw@scut.edu.cn

Ngai, T. E-mail: tongai@cuhk.edu.hk

¹ The authors contributed equally to this work.

Table of Contents

Experimental Procedures.....	3
Materials.....	3
pH-Responsive Performance of zein.....	3
pH-Responsive Performance of Emulsions Stabilized by zein.....	3
Synthesis of Au-loaded ZCPOPs (ZCPOPs-Au NCs).....	4
Physicochemical Characterization of ZCPOPs-Au NCs.....	4
Preparation and Characterization of Emulsions Stabilized by ZCPOPs-Au NCs.....	4
Catalytic reaction.....	4
HRP-Mimicking Property.....	5
The Processes of the Cascade Catalysis.....	5
Results and Discussion.....	6
Characterize phosphorylation of ZCPOPs.....	6
Reversible pH-responsive association-disassociation of ZCPOPs.....	7
pH-responsive emulsions stabilized by ZCPOPs.....	8
Working principle for pH-responsive emulsions stabilized by ZCPOPs.....	9
Recyclable interfacial catalysis.....	11
References.....	18

Experimental Procedures

Materials.

Zein (product Z 3625) was purchased from Sigma Chemical Co. (St. Louis, MO, USA). Phosphorus oxychloride was obtained from Saen Chemical Technology Co., Ltd. (Shanghai, China). Chloroauric acid trihydrate ($\text{HAuCl}_4 \cdot 3\text{H}_2\text{O}$, 47% Au base) and glucose were purchased from Aladdin Chemical Reagent Company (Shanghai, China). Ethyl acetate, sodium borohydride (NaBH_4) and p-nitroanisole were obtained from Lanzhou Institute of Chemical Physics (Lanzhou, China). Methyl phenyl sulfoxide and methyl phenyl sulfide were purchased from Aladdin Chemical Reagent Company (Shanghai, China). Glucose oxidase, Fluorescent dyes including Nile Red, Nile Blue A, and fluoresceine 5(6)-isothiocyanate mixed isomers (FITCs) were obtained from Sigma Chemical Co. (St. Louis, MO, USA), All other chemicals were of analytical grade.

pH-Responsive Performance of zein.

Preparation of phosphorylated zein. In a typical procedure, a stock solution of zein was prepared by dissolving 1.0 g zein in 40 mL ethanol (80% v/v). Then 1 ml of POCl_3 was slowly added into solution of zein under ice bath conditions. Furthermore, the pH of solution was maintained at 6.5-7.5 with 4M NaOH solution. The reaction was not complete until the pH reached a constant value. Subsequently, the above-reacted solution was dropped into 100 ml of deionized water, and excess ethanol was removed by rotary evaporation. The obtained solution was dialyzed in the presence of water for 48 h to remove impurities. Ultimately, the phosphorylated zein nanoparticles were achieved.

In brief, TEM observations were performed using a JEM-1400 Plus (JEOL Ltd, Japan) at an acceleration voltage of 120 kV. The sample (0.005-0.05 wt%) was dispersed in deionized water, and the pH of the solution was adjusted to 8.0, 4.3, or 4.2. A drop of the dispersion was spread onto 300 mesh copper grids coated with a carbon support film, and the specimens were then dried under vacuum for 5 h.

Morphological observations were also performed using a Merlin scanning electron microscope (Zeiss Co., Germany). The samples were dispersed in deionized water (0.05 wt%) under mechanical agitation at 600 rpm for 2 min. One drop of the dispersion was carefully placed on a glass slide and dried at room temperature. After that, the samples were coated with Au for conductivity and placed under the microscope for observation.

pH-Responsive Performance of Emulsions Stabilized by zein.

Typically, 10 mL of oil phase and 10 mL of a ZCPOPs suspension (0.2 wt%) were mixed in 25 mL glass vessels at room temperature. Emulsions were formed using an Ultraturrax T10 homogenizer (IKA, Germany) at a stirring rate of 15 000 rpm for 1 min. After standing at room temperature for 30 min, a few drops of HCl were added to adjust the pH to 3.8-4.2 to break up the emulsion. Slight magnetic stirring, stick stirring or hand shaking was used to facilitate the demulsification of the emulsions. The morphology of the emulsion was characterized using an optical microscope, a laser confocal microscope and a cryo-electron microscope.

ZCPs were prepared as a particulate emulsifier by an anti-solvent protocol. Typically, 10 mL of oil phase and 10 mL of a ZCPs dispersion (0.1 wt%, pH 8.0) were mixed in 25 mL glass vessels at room temperature, and the mixture was sheared using an Ultraturrax T10 homogenizer at a stirring rate of 15 000 rpm for 1 min. After incubation at room temperature for 30 min, a few drops of HCl were added to adjust the pH to 4.6-7.0 to break up the emulsions.

Cryo-SEM measurements were performed on a Hitachi S-480 instrument operating at 2.0 kV. Samples (emulsions) were frozen with liquid nitrogen and sublimated for 10 min at $-90\text{ }^\circ\text{C}$ to expose the sample structure. The surface of the sample was removed with a blade to facilitate observation of the interfacial structure and immediately measured.

CLSM images were recorded on a Leica TCS SP5 confocal laser scanning microscope (Leica Microsystems Inc., Heidelberg, Germany) equipped with a 20-HC PL APO/0.70NA oil-immersion objective lens. The samples were stained with a mixture of Nile blue (0.1%) and Nile red (0.1%). The stained samples were placed on concave confocal microscope slides and examined using a 630x magnification lens. The two dyes were excited with an argon/krypton laser and a helium/neon (He-Ne) laser at 488 nm and 633 nm, respectively.

An optical contact angle meter (OCA-20) with oscillating drop accessory ODG-20 (Dataphysics Instruments GmbH, Germany) was used to measure the adsorption kinetics of ZCPOPS solution at pH 8.0 and pH 4.8 (0.5 mg mL⁻¹). A drop of ZCPOPS solution (10 µL) was delivered by an inverted tip of syringe into an optical glass cuvette containing purified oil, and allowed to stand for 3 h to achieve adsorption at the oil-water interface. The drop image was photographed using the high-speed video camera, and the interfacial tension (γ) was calculated from the drop shape by Young–Laplace equation, as described in Güzey, Gülseren, Bruce, and Weiss (2006)^[1]. All the measurements were performed in duplicates at a room temperature of 25 °C. For each sample two consecutive measurements were performed, and each sample was replicated at least 2 times.

Synthesis of Au-loaded ZCPOPs (ZCPOPs-Au NCs).

Au NCs were deposited on ZCPOPs through the reduction of HAuCl₄ by NaBH₄ according to the method of Mahmoud et al^[31] with some modifications. In brief, HAuCl₄·3H₂O (10 mM, 2 mL) was added to 50 mL (0.2 wt%, pH 7.0) of a ZCPOPs suspension, and then 1 mL aliquots of freshly prepared ice-cold 10 mM NaBH₄ were added slowly to the mixing suspension until a stable brown-yellow colloid was observed. The suspension was left at room temperature for 24 h for stabilization. Au NP-labelled ZCPOPs was isolated by adjusting the pH to 4.3–4.5 and then centrifuging at 1000 rpm. The sediment was washed with deionized water until the supernatant was clear, the product was obtained.

Physicochemical Characterization of ZCPOPs-Au NCs.

TEM observations were performed using a JEM-2100 Plus (JEOL Ltd, Japan) at an acceleration voltage of 200 kV. The sample (0.05 wt%) was dispersed in deionized water and homogenized at 25 °C for 5 min. A drop of the suspension was spread onto copper grids coated with a carbon support film. After 1 min, excess liquid was blotted with filter paper, and the remaining film was allowed to dry for observation.

Atomic force microscopy (AFM) images were acquired on a Bruker Multimode instrument with a Quadrex Nanoscope 3D controller. Samples were prepared by adding one drop of proteinosome solution (0.02 wt%) onto a clean silica wafer and drying under vacuum for one day.

XPS spectra were recorded on a Kratos Axis Ultra DLD instrument, and the C_{1s} line at 284.6 e V was used as a reference.

The FT-IR spectra of the samples were recorded using a Perkin Elmer Spectrum RXIFT-IR Spectrometer (USA) at room temperature. The sample powder was blended with KBr powder and pressed into tablets before spectra were obtained over the range of 4000 to 500 cm⁻¹ at a resolution of 8 cm⁻¹.

The UV-Vis spectra of Au NCs-ZCPOPs were recorded by Nano Photometer N60 instrument (IMPLEN, Germany).

XRD data of the samples were obtained with a RU200R X-ray diffractometer (Rigaku, Tokyo, Japan) by using Cu K α radiation at 35 kV and 20 mA, a theta-compensating slit, and a diffracted beam monochromator in a range of $2\theta = 25\text{--}65^\circ$.

Au and P content were analyzed with an inductively coupled plasma-atomic emission spectrometry (ICP-AES, Atom Scan16, TJA Co.). An aliquot of sample (10 mg) was taken, and 5 mL of nitric acid and 1 mL of hydrogen peroxide were added, and the mixture was heated on a hot plate at 300 °C for digestion.

Preparation and Characterization of Emulsions Stabilized by ZCPOPs-Au NCs.

Typically, 10.0 mL of oil phase and 10.0 mL of ZCPOPs-Au NC suspensions (1 mg/mL) were mixed in 25 mL glass vessels at room temperature. Emulsions were formed using an Ultraturrax T10 homogenizer (IKA, Germany) at a stirring rate of 15 000 rpm for 1 min.

CLSM images were recorded on a Leica TCS SP5 confocal laser scanning microscope (Leica Microsystems Inc., Heidelberg, Germany) equipped with a 20-HC PL APO/0.70NA oil-immersion objective lens. The samples were stained with Nile red (0.1%). The stained samples were placed on concave confocal microscope slides and examined using a 630x magnification lens. The dye was excited with an argon/krypton laser and a He-Ne laser at 488 nm.

Catalytic reaction.

Ethyl acetate (10 mL) containing p-nitroanisole (4 mM) and ZCPOPs-Au NCs aqueous solution (10 mL) were added to a clean plastic vial at room temperature. Then, a few drops of NaOH solution (1 M) were added into this system to adjust the pH to 8.0-8.5. Emulsions were formed by homogenization using an Ultraturrax T10 homogenizer (IKA, Germany) at a stirring rate of 15 000 rpm for 1 min. Excess NaBH₄ aqueous solution was added to the emulsions with gentle stirring. Hydrogenation was conducted under stirring at room temperature for a given time. After the reaction, a known volume of HCl (1 M) aqueous solution was added to the emulsion to break it up. After complete phase separation, the resulting extra upper oil phase was carefully isolated by decantation. The yield was determined with a 7890B gas chromatograph (Agilent Technologies Co., China). For the next reaction cycle, fresh solvent and substrate were added to the residual water phase. A few drops of NaOH solution were added to the above system to adjust the pH to the basic range. After homogenization, emulsions stabilized by ZCPOPs-Au NCs formed again. The other procedures for the reaction and catalyst recycling were the same as those used in the first reaction cycle.

HRP-Mimicking Property.

Considering TMB can be oxidized by H₂O₂ to generate colored product (TMB⁺) in the presence of the peroxidase mimetics (H₂O₂+TMB→H₂O+TMB⁺), TMB was used as a typical substrate to evaluate the catalytic properties of ZCPOPs-Au NC. In a typical procedure, 2.5 mL of solution included 1 mL of purified ZCPOPs-Au NC (0.2%), 1 mL of 2 mM TMB and 0.5 mL of 100 mM H₂O₂ were added sequentially into a 5mL tube. later, the absorption spectra were recorded using a Implen NanoPhotometer C40 spectrophotometer. For studying the effects of pH and time on HRP-mimicking property, the same procedures were repeated only the pH medium and time was changed correspondingly.

The Processes of the Cascade Catalysis.

The emulsion system was prepared by dissolving 3.47mmol glucose in 2.5 mL ZCPOPs-Au NC solution (0.2%, 0.05 M PBS), followed by adding 2.5 mL ethyl acetate (containing 5mM methyl phenyl sulfide). After stirring, the stable emulsions were obtained, and reaction was initiated by adding 6mg GOx. Two-phase: Glucose was dissolved in 2.5 mL ZCPOPs-Au NC solution (0.2%, 0.05 M PBS), followed by adding 2.5 mL ethyl acetate (containing 5mM methyl phenyl sulfide), and reaction was initiated by adding 6mg GOx.

Results and Discussion

Characterize phosphorylation of ZCPOPS

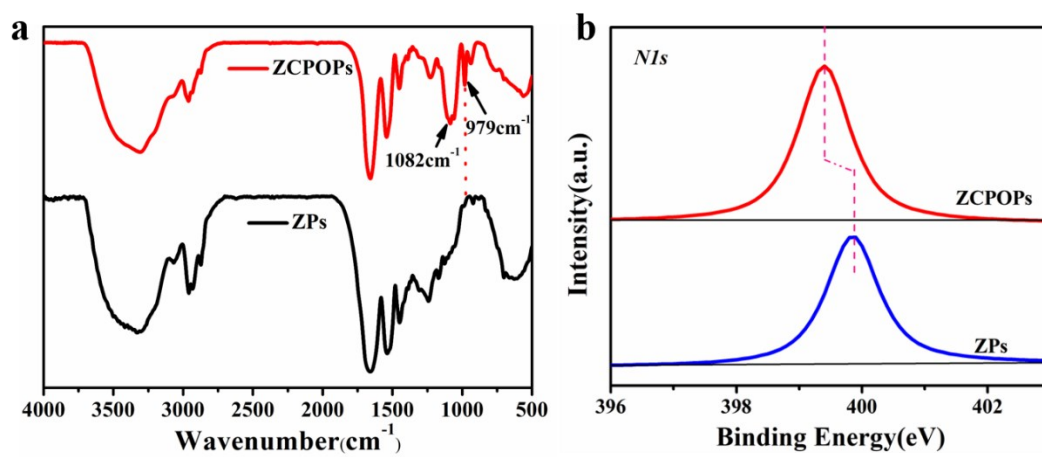


Fig. S1. FTIR (a) spectra and XPS spectra (b) of the ZCPs and ZCPOPs.

Reversible pH-responsive association-disassociation of ZCPOPs

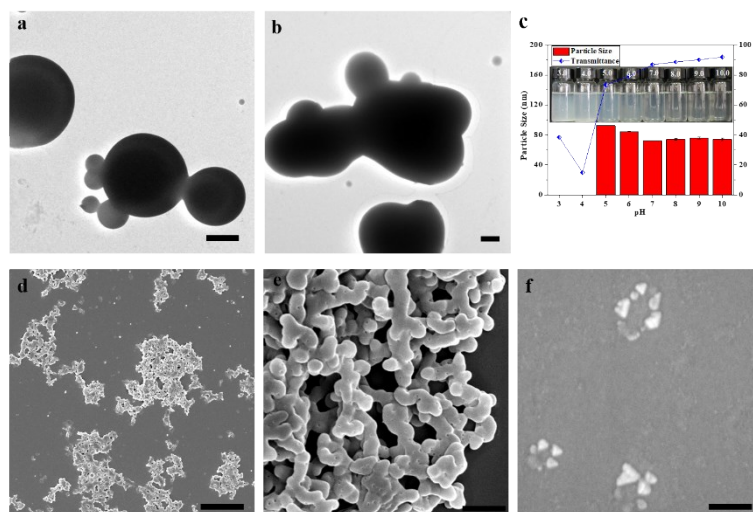


Fig. S2. TEM image of ZCPOPs at 4.3(a) and 4.2(b), scale bar, 1 μ m. (c) Particle size and transmittance %T of ZCPOPs as a function of pH. SEM images of ZCPOPs (0.05 wt%) (d e), scale bar, 10 μ m and 1 μ m. ZCPOPs was diluted by 5 times from 0.05 wt% to 0.01 wt% by magnetic stirring (f), and the pH of ZCPOPs solution remained constant (pH 4.2), scale bar 0.2 μ m. Interestingly, the intermediate colloidal architecture at pH 4.2 returned to the uniformed particles with size of 60 nm after the dilution by 5 times.

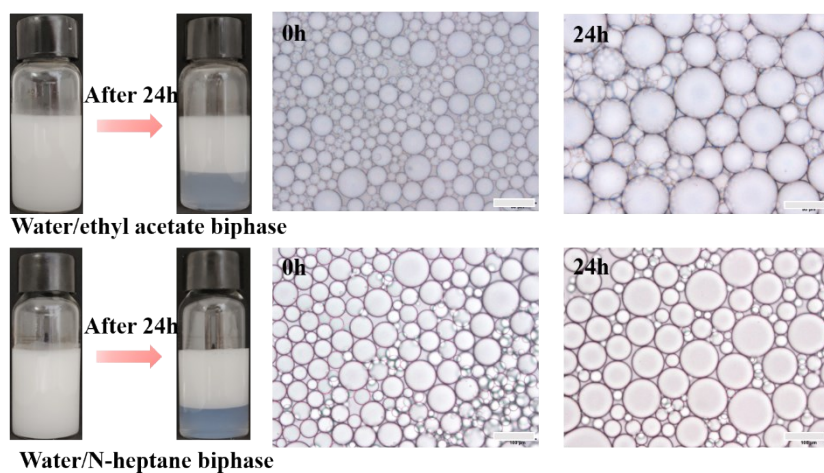


Fig. S3. Pickering emulsions stabilized by ZCPOPs. Appearance and optical micrographs of ZCPOPs-stabilized emulsion (0.2 wt%) at 0h and 24h using different oil, scale bar 50 μ m. A typical oil-in-water (o/w) Pickering emulsion with equal volume fractions of oil/water was prepared by shearing the mixtures at a stirring rate of 15 000 rpm for 1 min. As shown in **Figure S3**, the size of the emulsion droplets is in the range of 10–50 μ m. After storage for 1 day, the droplet size did not change obviously, which indicated that the prepared emulsions are stable against coalescence. And yet, the serum volume fraction increased rapidly during the first days. The serum volume fraction, after that, remained unchanged for the next two weeks.

pH-responsive emulsions stabilized by ZCPOPs.

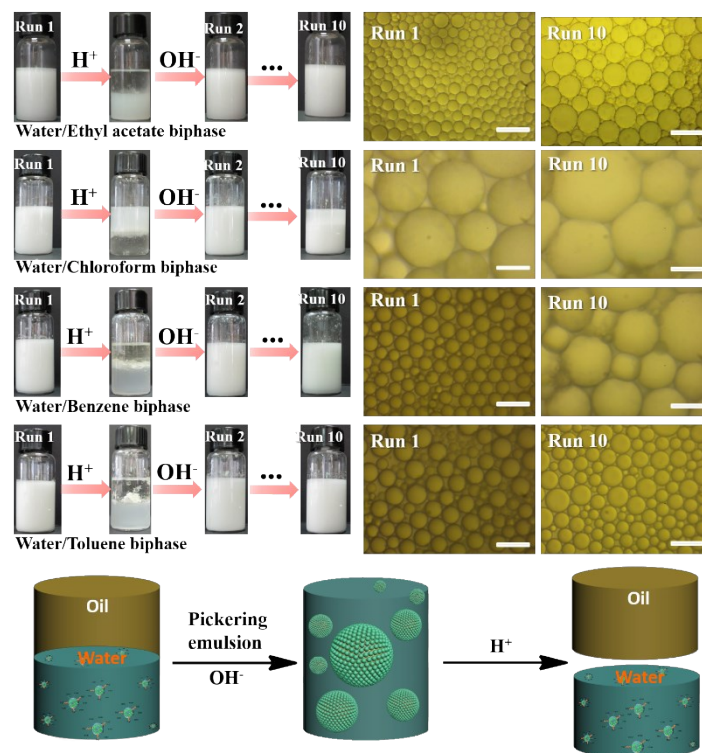


Fig. S4. pH-responsive emulsions stabilized by ZCPOPs. Appearance and optical micrographs of successive pH-responsive ZCPOPs-stabilized emulsion (0.2 wt%) inversion cycles using different oil (1st, 2nd and 10th cycle). After addition of an equal volume of oil phase into water containing 0.2 wt % of the sample (with respect to water), and subsequent homogenizing at a rate of 15 000 rpm for 1 min, different phenomena were observed for these samples. The as-prepared emulsion stabilized by ZCPOPs was stable at pH 8.5, and complete macroscopic phase separation occurred within 1 min upon adjusting the pH to 3.8-4.2. This system, however, rapidly restored the emulsion (o/w) when a few drops of NaOH solution were added and the pH of the water phase was adjusted to 8.5. Remarkably, this emulsion could be reversibly switched on and off over 10 cycles. Scale bar, 30 μm .

Working principle for pH-responsive emulsions stabilized by ZCPOPs

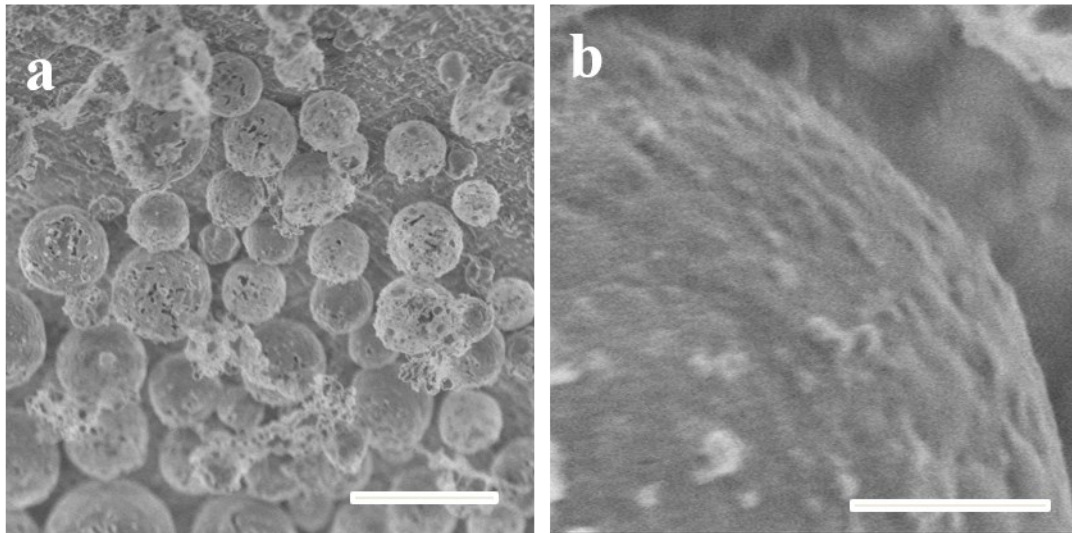


Fig. S5. Cryo-SEM images of ZCPOPs-stabilized emulsions at pH 8.5 (a, b) using ethyl acetate as oil phase. scale bar 10 μ m (a) and 1.5 μ m (b).

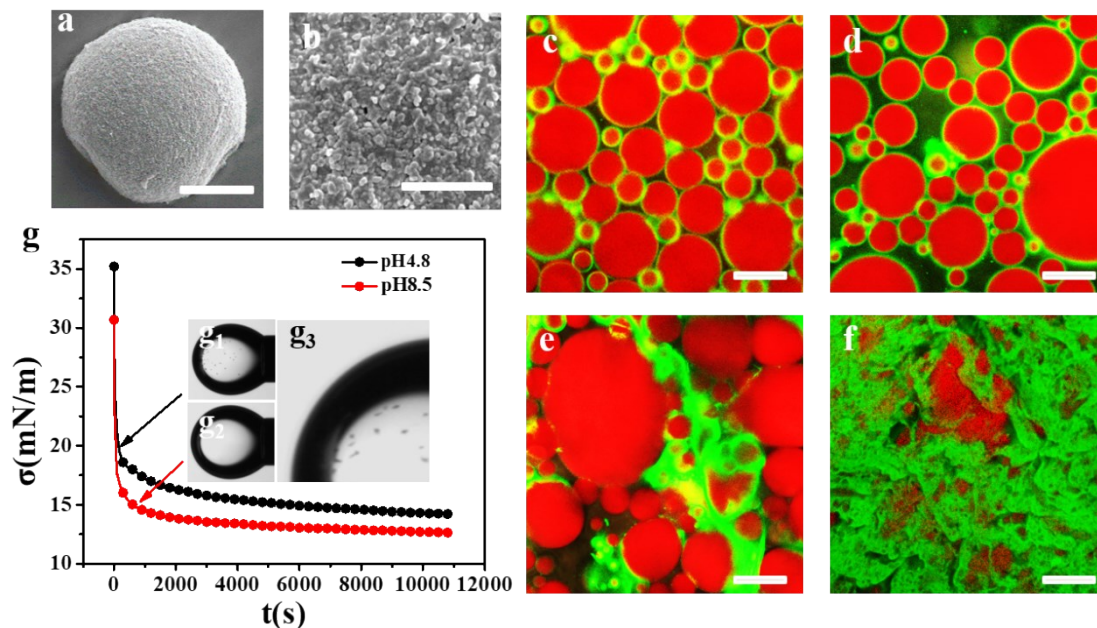


Fig. S6. Mechanism of pH-responsive emulsions stabilized by ZCPOPs. (a-b) SEM image of emulsion droplets at pH 8.5, scale bar, 10 μ m and 1 μ m. (c-f) CLSM image of ZCPOPs-stabilized emulsions using dodecane as the oil phase at pH 8.5, 6.0, 5.0 and 4.0, scale bar, 20 μ m. (g) The change in interfacial tension with time using dodecane as the oil phase at different pH (g₁, g₂). Droplet images of ZCPOPs solutions at different pH values. A large number of flocs were present in the droplets at pH 4.8 (g₃). SEM and CLSM were used to reflect the dynamic process of the emulsion droplet interface structure under pH stimulation. For the emulsions at pH 8.5, the spherical outer shells presented a close-packed array of nanoparticles (with size of 60-100nm, **Figure S6a,b**). Under the pH 8.5, small droplets with complete interface layer were clearly visualized, reflecting that droplets have higher interface coverage (**Figure S6c**). As the pH was shifted to 5.0 and 4.0 (**Figure S6e, f**), lots of aggregates of emulsifiers appeared in the aqueous phase. To gain more insight, we conducted the interfacial adsorption for ZCPOPs at different pH. As depicted in **Figure S6g**, ZCPOPs had different interfacial tension (14.20 and 12.63 mN m⁻¹) and adsorption rates (1.29 and 1.67 mN m⁻¹S^{-0.5}) at pH 4.8 and 8.5. The behavior of the interfacial adsorption makes us conclude that demulsification is associated with reduced interfacial activity of the emulsifier.

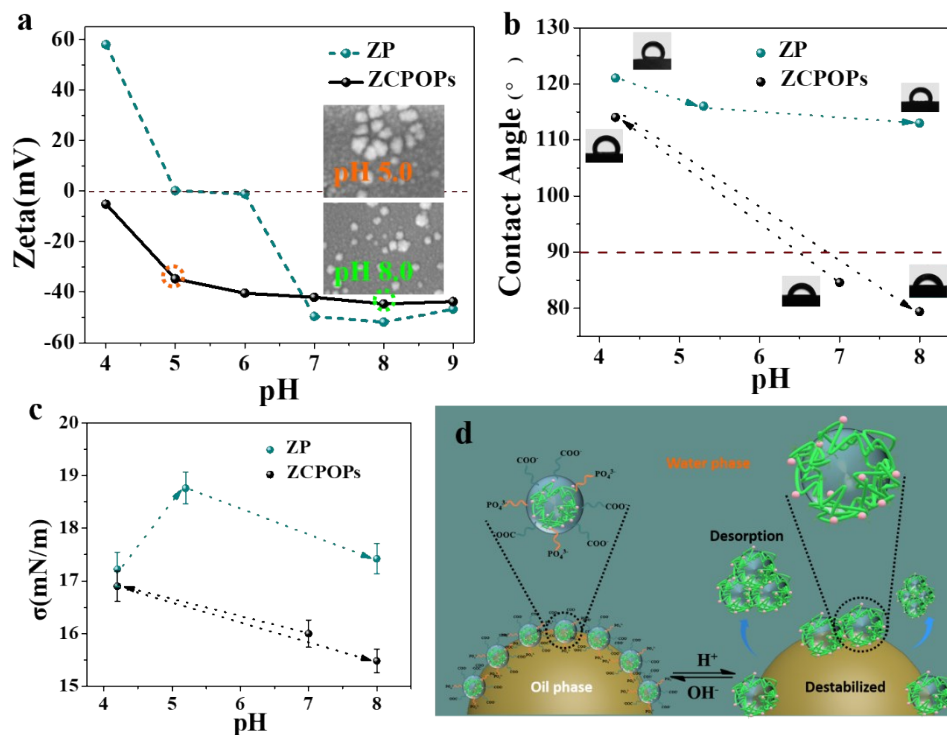


Fig. S7. (a) Zeta potentials of nanoparticles at different pH values, three phase contact angles (b) and interfacial tension (c) of nanoparticles treated with different pH value water. (d) A schematic representation of pH-responsive emulsions stabilized by ZCPOPs.

The emulsion-inversion ability is related to the detachment obstacles of nanoparticles. It is commonly known that the energy ΔG_{detach} required to remove a solid spherical particle from the oil-water interface is calculated using the following eq. (1).

$$\Delta G_{detach} = \pi R^2 \gamma_{ow} (1 - |\cos \theta|)^2$$

where R is the particle diameter, γ_{ow} is the tension of the oil-water interface, and θ is the three-phase contact angle. As known from equation (1), particle size and wettability are the key factors to control the ΔG_{detach} . As shown in **Figure S7**, under the neutral conditions, the phosphate deprotonation made ZCPOPs surface hydrophilic because of its bearing charge. Therefore, the three-contact angle is maintained at 84.6°. Furthermore, the interfacial tension of ZCPOPs was kept at 16mN/m⁻¹, which endowed higher ΔG_{detach} for particles. As the pH decreased to 4.2 (its isoelectric point, the zeta potential particles were measured to be approximately 0), the three-phase contact angle of particles is greatly increased to 114°, the results are in good consistent with the observed decrease of interfacial activity. This may be explained by the protonation of amine which makes the surface of the ZCPOPs hydrophobic. As a result, the interface desorption energy is reduced. In addition, particles in interface or aqueous phase aggregate into micron-sized clusters (**Figure S6e, f**) because of the increased hydrophobicity of the particles and the weakening of the electrostatic repulsion at this time. More seriously, the coalescence of the emulsion causes the separation of the oil phase and the aqueous phase due to the exposure of the droplet interface.

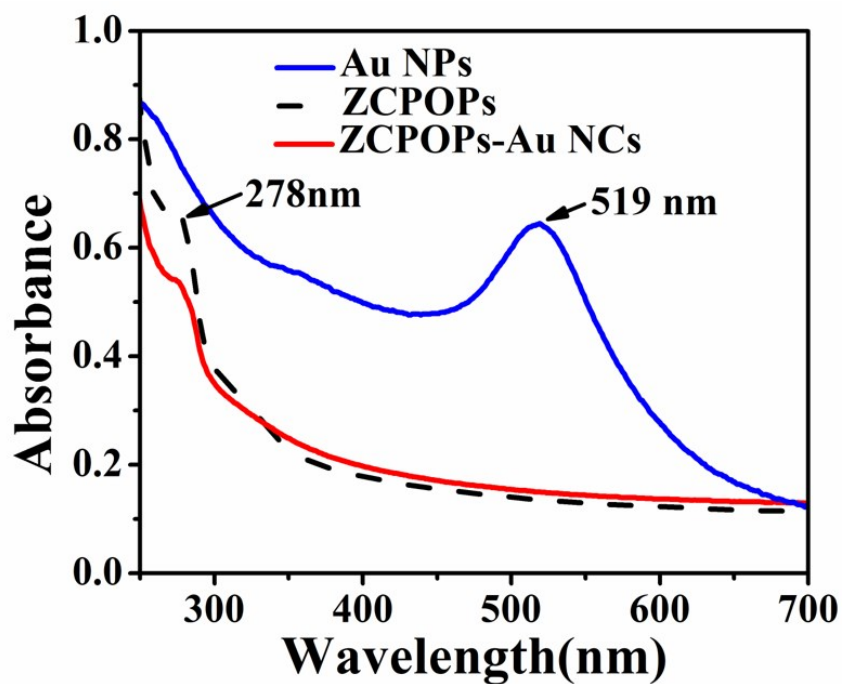


Fig. S8. The maximum UV-vis absorbance at 278 nm belonged to ZCPOPs, and the gold nanoparticles had an absorption peak at 519 nm.

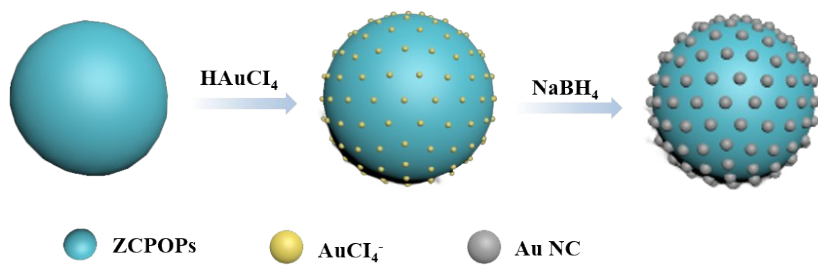


Fig. S9. Schematic representation of possible mechanisms for the formation of ZCPOPs-Au NCs

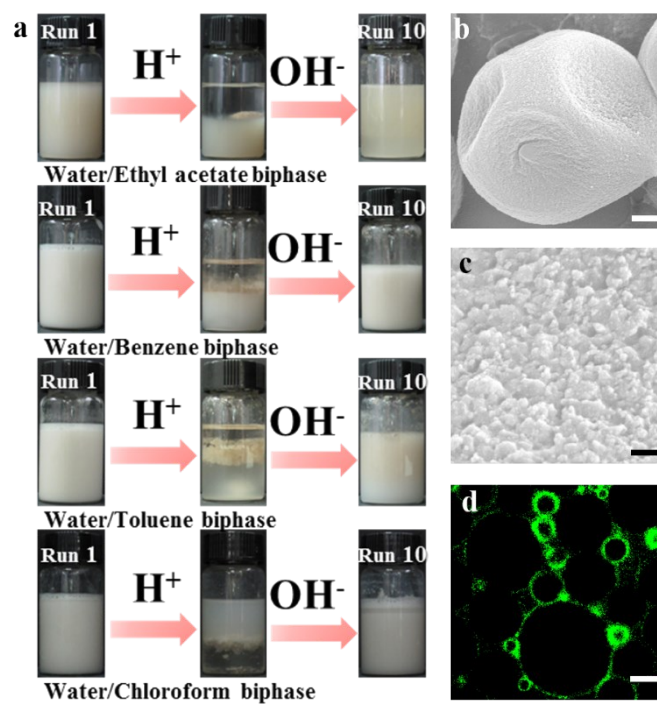


Fig. S10. Photographs of pH-responsive ZCPOPs-Au NC-stabilized emulsion with different oil phase (a). SEM (b, c) and CLSM (d) of successive pH-responsive ZCPOPs-Au NCs-stabilized emulsion. Scale bar, (b) 2 μ m, (c) 200nm and (d) 25 μ m.

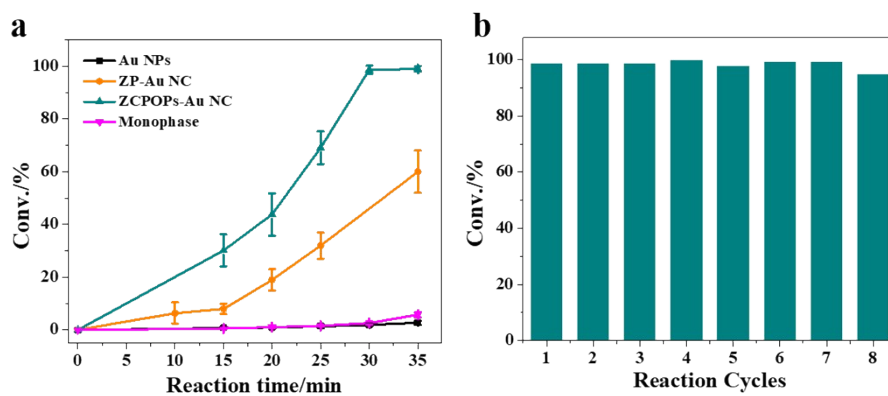


Fig. S11. (a) Conversion versus reaction time curve for p-nitroanisole hydro-genation. Monophase system: p-nitroanisole and ZCPOPs-Au NCs were immersed in only ethyl acetate and stirred at 300 rpm for reaction. Au NPs system: the oil and water phase were mixed by stirring at 300 rpm. Pickering emulsion system: emulsion was stabilized by ZCPs-Au NCs or ZCPOPs-Au NCs at pH 8. (b) Recycling of ZCPOPs-Au NCs catalyst using p-nitroanisole hydrogenation as model reaction.

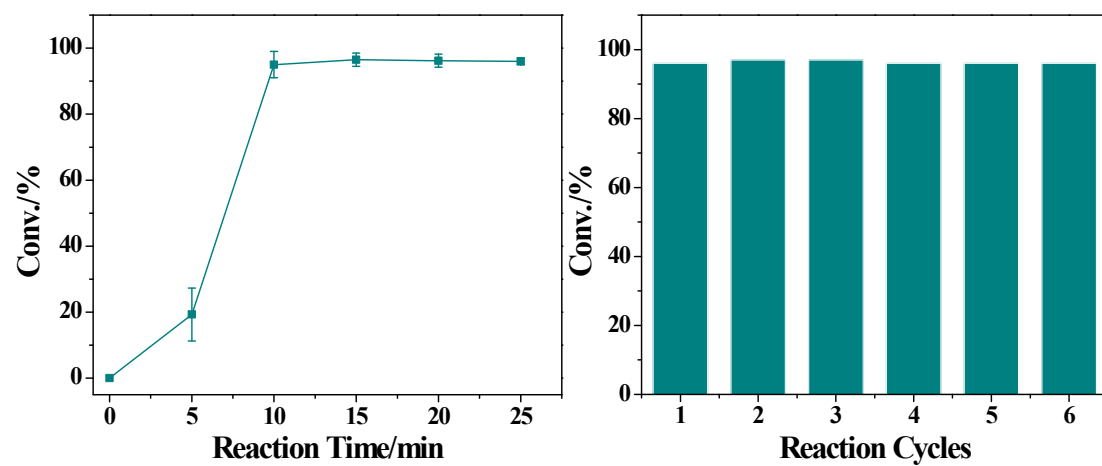


Fig. S12. The recycling results of catalyst reaction for ZCPOPs-Au NCs using chloroform as oil phase (right) and corresponding reaction profiles (left).

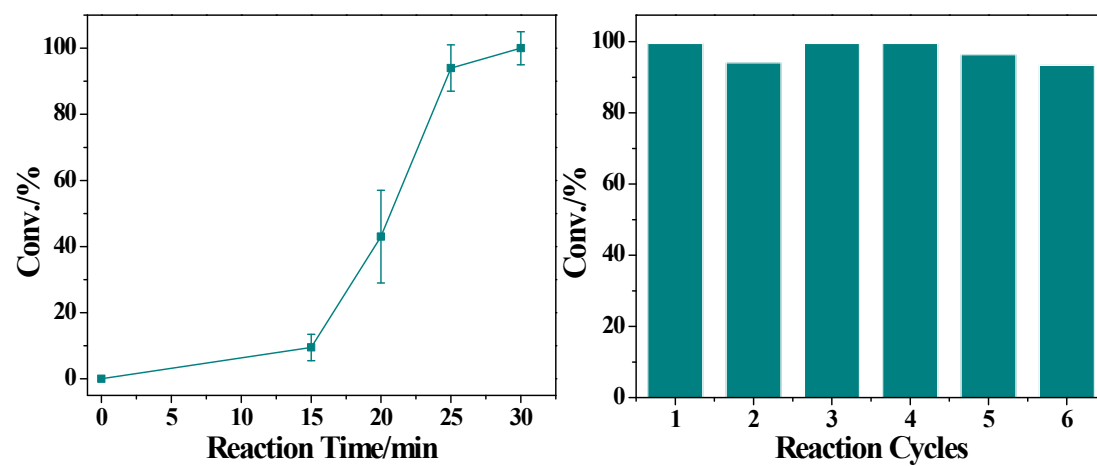


Fig. S13. The recycling results of catalyst reaction for ZCPOPs-Au NCs using toluene as oil phase (right) and corresponding reaction profiles (left).

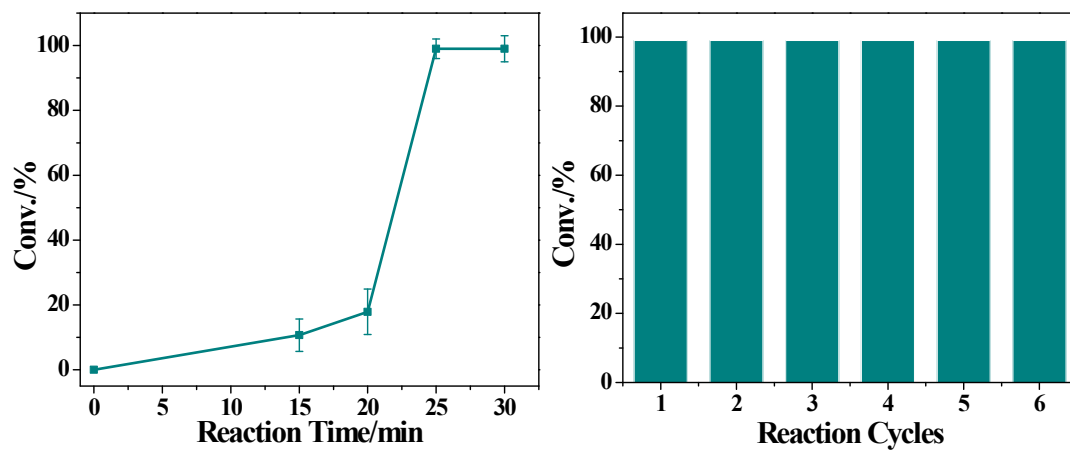


Fig. S14. The recycling results of catalyst reaction for ZCPOPs-Au NCs using benzene as oil phase (right) and corresponding reaction profiles (left)

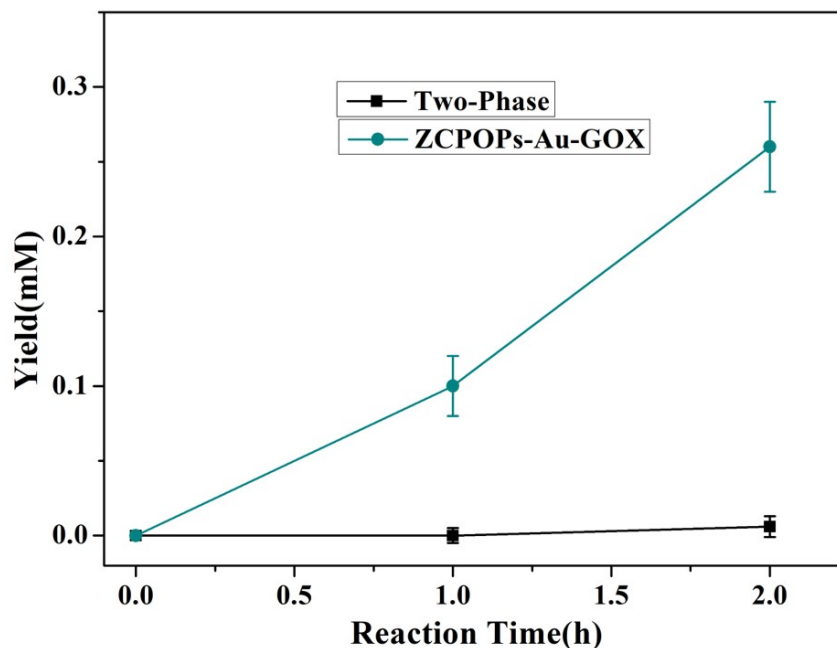


Fig. S15. Activity comparison between GOx-Au NCs PIC cascade reactions and two-phase system as a function of reaction times. Two-phase: Glucose was dissolved in 2.5 mL ZCPOPs-Au NC solution (0.2%, 0.05 M PBS), followed by adding 2.5 mL ethyl acetate (containing 5mM methyl phenyl sulfide), and reaction was initiated by adding 6mg GOx. Pickering emulsion system: The emulsion system was prepared by dissolving 3.47mmol/L glucose in 2.5 mL ZCPOPs-Au NC solution (0.2%, 0.05 M PBS), followed by adding 2.5 mL ethyl acetate (containing 5mM methyl phenyl sulfide). After stirring, the stable emulsions were obtained, and reaction was initiated by adding 6mg GOx. As observed from **Figure S15**, after 2h, the Pickering reaction system achieved 260 μ M yield of methyl phenyl sulfide, but almost no product was detected in the two-phase reaction system. Impressively, Pickering system gave rise to over 65-fold higher efficiency than two - phase system. The higher efficiency of the Pickering reaction over the two-phase reaction may be attributed to the presence of the higher interface formed upon addition of the Pickering reaction system. The excellent performance achieved by ZCPOPs-Au-Gox in Pickering emulsion further demonstrates the significance of the oil-water interface in catalysis.

Table S1 The dependence of pH-responsive transition on the interfacial characteristics and polarity of various oils

Oil phase	γ_{ow} (mN m ⁻¹)	Polarity	Transferable
N-Hexane	51.1	0.06	Yes
N-Heptane	49.4	0.2	Yes
Dichloromethane	44.3	3.4	Yes
Petroleum ether	42	0.01	Yes
Toluene	35.7	2.4	Yes
Benzene	35	3	Yes
Ethyl acetate	19.8	4.3	Yes
N-Butanol	1.8	3.7	Yes

References

- [1] Y. Xi, B. Liu, H. Jiang, S. Yin, T. Ngai and X. Yang, *Chemical Science*, 2020, 11, 3797-3803
- [2] Y. B. Chen, X. F. Zhu, T. X. Liu, W. F. Lin, C. H. Tang, R. Liu, *Food hydrocolloids*, 2019, 87, 404-412.
- [3] C. Qi, J. Liu, Y. Jin, L. Xu, G. Wang, Z. Wang, L. Wang, *Biomaterials*, 2018, 163, 89-104.
- [4] Y. Xi, Z. Luo, X. Lu, X. Peng, *Journal of Agricultural and Food Chemistry*, 2018, 66, 228-237
- [5] D. Güzey, I. Gülseren, B. Bruce, J. Weiss, *Food Hydrocolloid*, 2006, 20, 669-677.
- [6] Y. Xi, Y. Zou, Z. Luo, L. Qi, and X. Lu, *Journal of Agricultural and Food Chemistry*, 2019, 67, 1931–11941.
- [7] K. A. Mahmoud, K. B. Male, S. Hrapovic, J. H. Luong, *ACS Appl. Mater. Inter.* 2009, 1, 1383-1386.
- [8] X. Cui, J. Wang, B. Liu, S. Ling, R. Long, Y. Xiong, *J. Am. Chem. Soc.* 2018, 140, 16514-16520.
- [9] Y. H. Kuan, R. Bhat, A. A. Karim, *J. Agric. Food chem.* 2011, 59, 4111-4118.